Construction and Building Materials 321 (2022) 126330

Contents lists available at ScienceDirect

Construction and Building Materials

journal homepage: www.elsevier.com/locate/conbuildmat

Thermal performance characterization of cement-based lightweight blocks incorporating textile waste

Ana Briga-Sá [a,*], Norma Gaibor [b], Leandro Magalhães [c], Tiago Pinto [d], Dinis Leitão [e]

[a] CQ-VR and ECT- School of Science and Technology, University of Trás-os-Montes e Alto Douro, 5000-801 Vila Real, Portugal
[b] Department of Civil Engineering, School of Engineering of the University of Minho, Azurém Campus, 4800-058 Guimarães, Portugal
[c] Polytechnic Institute of Bragança, 5300-253 Bragança, Portugal
[d] C-MADE and ECT- School of Science and Technology, University of Trás-os-Montes e Alto Douro, 5000-801 Vila Real, Portugal
[e] CTAC, Department of Civil Engineering, University of Minho, 4800-058 Guimarães, Portugal

ARTICLE INFO

Keywords:
Lightweight blocks
Textile waste
Thermal performance
Experimental work
Sustainability
Building materials

ABSTRACT

Textile industry is one of the most important sectors of the global economy, but at the same rate as production, millions of tons of textile waste (TW) are generated worldwide, causing negative impacts on the environment. To mitigate CO_2 emissions and TW landfilled, its reuse and recycling are considered promising in fulfilling the circular economy principles. Furthermore, its valorization as building materials components may be a contribution towards sustainable construction. Studies already developed in this domain demonstrate that more research work is needed so the suitability of TW as building insulation materials can be assessed. In this context, it is intended with the research work here presented to propose cement-based lightweight blocks (LWB) incorporating TW and discuss their application as insulation materials purposes.

The studied TW was fabric leftovers from the textile industry, constituted by 70 % wool, 25% viscose, and 5% elastane. TW percentages of 6.25%, 8.16%, and 8.75% were considered in the cement mixture composition of LWB1, LWB2 and LWB3, respectively, and their influence on the LWB thermal performance was analyzed. The LWB thermal performance characterization was carried out by analyzing heat fluxes, inner surface temperatures, thermal transmission coefficients, and infrared thermal imaging. The obtained results revealed their suitability for thermal insulation applications. Values of 0.34 m^2°C/W, 0.61 m^2°C/W, and 0.67 m^2°C/W were estimated for the thermal resistance of LWB1, LWB2 and LWB3, respectively, achieving higher thermal stability when higher percentage of TW is incorporated in the cementitious mixture composition. A comparison of the LWB with currently available building materials, such as simple masonry walls and insulating concrete forms, was also performed showing promising results for the proposed textile waste-based materials.

1. Introduction

Textile industry is one of the most important sectors of the global economy, being distributed throughout Europe but more intensely in some European Union (EU) countries. Italy is the main European producer, followed by Germany, UK, France, and Spain. These five countries account for over 80% of textile companies in the EU [1]. In Portugal, textile industries are mainly located in the north of the country, having an outstanding position in the economy and businesses, with over 150 years of large-scale production, being the most important sector in the foreign trade balance [2]. On the other hand, textile industry has been causing negative impacts on the environment, specifically in what concerns to the Greenhouse Gases (GHG) emissions, since per 1 ton of textile production 17 tons of CO_2 are generated [3]. Thus, at the same rate as production, millions of tons of textile waste (TW) are produced worldwide, whose amount varies from region to region depending on the culture, population density, living style, fashion trends, and users income [4].

Textile waste can be either postindustrial or postconsumer [5]. Postindustrial TW is the waste generated during the manufacturing process and usually involves apparel cutting waste, excess fabrics, and refusals due to quality issues. It is known as 'clean waste' since fabrics are unused when disposal. Postconsumer TW refers to the unwanted clothing discarded by the consumer after being used [6,7]. By 2030, the waste production sectors will have risen by 63% [8], with TW representing approximately 6% of the total municipal solid waste (MSW) and

* Corresponding author.
E-mail address: anas@utad.pt (A. Briga-Sá).

https://doi.org/10.1016/j.conbuildmat.2022.126330
Received 1 October 2021; Received in revised form 29 December 2021; Accepted 3 January 2022
Available online 10 January 2022

accounting for more than 3% of the GHG emissions [9]. In the United States, about eleven million tons of textile affiliated products end up in landfills [10], while in the EU, post-consumer textile waste is registered at nearly 16 million tons yearly. In addition, only 10% of this waste is recycled by industrial enterprises [11], and other 15–25% of disposed textiles are collected by other means (the rest is landfilled or incinerated), whereof about 50% is down cycled and 50% is reused, mainly through exporting to developing countries [7,12]. Nevertheless, there are considerable disparities within Europe. More notable examples are Germany and Denmark, in which about 70% and 50% of disposed textiles are, respectively, collected for reuse and recycling [13]. In Portugal, the main TW becomes from wool, cotton, and synthetic and artificial fibers, according to the Technical Guide of the Textile Sector [14]. The TW annual generation in this country is about 230 tons, which represents 5% of MSW [15].

From the environmental point of view, as most of the disposed textiles products can be reused and recycling, which means about 83–85%, it represents a diminishing impact compared to incineration and landfilling [13]. Statistically, TW represents about 5% of the volume in a landfill and the global textile recycling rate stands for approximately 13%. This is relatively low comparing to other materials, which achieve much higher recycling rates, e.g., 58% for paper, 73% for ferrous wastes and 90% for glass containers [10]. However, reuse is more advantageous than recycling, mainly because some types of waste contain many of toxic materials and heavy metals (e.g. Pb, Cr, Hg, Ni, etc.) deriving from textile dyes [9]. Thus, environmental concerns with waste resulting from textile industry have been increasing. In the EU, various directives and regulations are in practice when it comes to the management, treatment, and disposals of waste materials, such as the Waste Framework Directive (EU, 2008) [16], the Landfill Directive (EU, 2003, EU, 1999) [17,18], and the Waste Incineration Directive (EU, 2000) [19]. These directives have been rapidly transforming the waste management systems and pushing EU countries to adopt the legislative incentives in more sustainable ways, towards environment protection and human health, for instance, rising the recovery of valuable resources and decreasing the disposal in landfills [20].

Based on the economic assessment of TW streams, this type of wastes can be a material source for the generation of value-added products. Due to the periodic generation of TW, its reuse and recycling are considered promising in fulfilling the concept of circular economy [21]. A In this context, adding this type of wastes as building materials components can be a promising solution, contributing to the reduction of energy consumption employed in the exploitation of natural resources, performing a significant role in sustainability, including the environmental, economic, and social perspectives [22,23]. However, according to the literature review, few studies have been developed in this field, justifying more research work, namely with emphasis on obtaining building materials with thermal insulation capacity by incorporating TW.

Textile waste as an alternative thermal insulation building material solution was researched by Ana Briga-Sá et al. [24], finding that the thermal reinforcement of external double walls with woven fabric waste (WFW) and woven fabric sub-waste (WFS) in the air-box increased the thermal resistance of the wall in 56% and 30%, respectively, when compared to the double-wall with the empty air-box. It was also concluded that WFW has better insulation characteristics than WFS. The thermal conductivity (λ) value obtained for the WFW is similar to the ones that characterize the well-known thermal insulation materials, such as extruded polystyrene (XPS), expanded polystyrene (EPS), and mineral wool (MW). Even so, similarities were found with other insulation materials such as granules of clay, vermiculite, or expanded perlite. Dissanayake et al. [25] studied the development of thermal insulation panels using compression molding. Different proportions of Nylon/Spandex and Polyurethane were subjected to a thermal conductivity test. A panel of 1 m^2 with 10 mm of thickness was produced using 10 kg of waste material. The mixture presenting the best thermal insulation was experimentally found to be 60% Nylon/Spandex fabric shreds mixed with 40% Polyurethane shreds, achieving a thermal conductivity value of 0.0953 W/m K. It was also presented that the thermal conductivity value can be approximately described in the form $1367 * T^{-5.272} + 0.08799$, where T represents the thickness of the panel. Gounni et al. [26] investigated the thermal performance of an external wall based on acrylic and wool TW and submitted it to real climatic conditions tests. Results showed a good thermal behavior, characterized by a thermal conductivity varying in the range 0.03745–0.04581 W/m K. The experimental results were validated using a thermally controlled cavity at a reduced scale. A comparison of the thermal and energetic performance of the wall incorporating the proposed material and the classical insulation materials (i.e., rock wool (RW) and EPS)) was performed, showing that the TW-based insulation is a competitive solution in terms of annual heating and cooling loads. Islam et al. [27] discussed the mechanism of thermal and acoustic insulation of TW through the measurement process by following the international standards. The insulation properties of different materials were compared. In some cases, thermal and acoustic insulation materials produced from TW showed much more favorable results than the currently available and dominating products in the market. Considering the promising thermal performance of textile waste-based materials, a more detailed characterization of the TW potential should be performed. Several solutions can be proposed for insulation purposes, considering the amount and diversity of TW generated. More research work can be done aiming to fully characterize new TW-based insulation products with different mixtures compositions, by replacing commonly used materials for TW and applying different binders. It is intended with the research work here presented to contribute to the scientific knowledge in this field, evaluating the potential of incorporating TW to produce lightweight blocks (LWB) with insulation purposes. Three cement-based LWB with different TW compositions will be thermally characterized. Different thermal parameters such as heat fluxes, inner surface temperatures, thermal transmission coefficient, thermal resistance and thermal conductivity will be estimated and discussed. An infrared thermal imaging analysis will be performed to assess the inner and outer surface temperatures fluctuation. A comparison with current insulation materials will also be done to evaluate the suitability of the proposed textile waste-based materials. This research work constitutes a preliminary approach of applying this type of textile wastes as cement-based lightweight blocks with insulation properties, aiming to be an incentive to waste reuse as sustainable materials components, fitting the circular economy principles.

2. Materials and methods

2.1. Textile waste (TW) characterization

The TW used in this work was provided by a Portuguese textile factory. The original size of the TW pieces was considered to large (10 to 15 cm) to be incorporated in cementitious mixtures, so they were subsequently cut into smaller pieces with a maximum length of 3 cm in order to facilitate both the workability and molding of the lightweight block's mixtures. (Fig. 1).

The density of dry pieces and water absorption of TW were determined following NP EN 1097-6 (Annex A and C) [28]. The experimental procedure was replicated three times and the average and coefficient of variation were calculated. It was concluded that TW presented low density, 217 kg/m^3 (CoV: 0.21), being also characterized by a high-water absorption, 892.60% (CoV: 0.07) in comparison with other types of wastes [29,30], as it was expected.

In order to identify the TW composition, a DHT-2 KFG moisture meter was used, Fig. 2. This device instantly measures the moisture content of fibers, yarns, and textiles, allowing to obtain, on a scale from 0 to 100, the textile composition, the percentages of cotton, wool, linen, polyester, and acrylic fibers, among others. The moisture content is determined using needle probes that measure the electrical conductivity

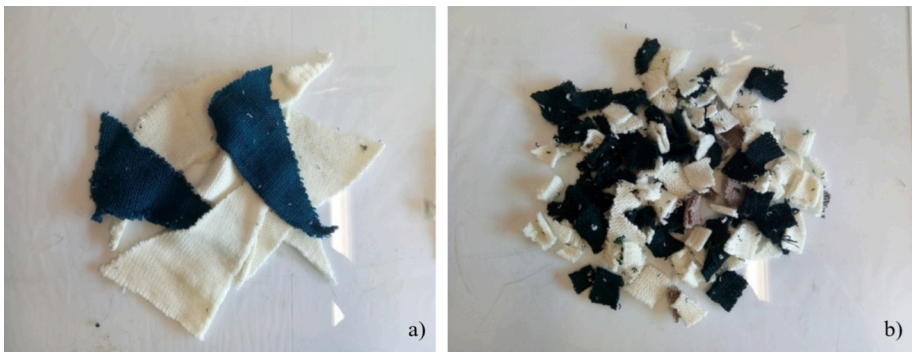

Fig. 1. Textile waste incorporated in the lightweight blocks mixtures: a) Original dimensions, b) After being cut (max 3 cm length).

Fig. 2. DHT-2 KFG moisture meter.

of the material, which is always proportional to the content of the moisture, allowing to identify its composition. Thus, it was concluded that the TW under study is composed of 70% wool, 25% viscose, and 5% elastane.

Among the natural fibers, wool from animals (sheep) is one of the oldest textile fibers used by mankind [28], known to have many outstanding properties including excellent insulation and low flammability characteristics [29,27]. One of the disadvantages associated with the animal wool insulation materials is their susceptibility to higher moisture content, evidenced in the water absorption content of the TW used in this study, and the resultant drop in their performance [30]. In terms of environmental profiles, wool fiber-based materials consume the lowest amount of energy during the material use and disposal stages than any other existing natural materials [31]. Viscose fiber is widely used in clothing due to its comfort and good dying properties, but the flammability limits its application [32]. A viscose fiber can be described as a fiber bundle consisting of thin, round fibers, which create grooves on the surface of the bundle. It presents a high water retention capacity and a high level of swelling [33]. Elastane fibers are filaments of which at least 85% by weight consist of segmented polyurethane (urea), characterized by high elasticity and, at the same time, high strength values, balanced elastic properties, and excellent thermal and hygrothermal behavior [34].

2.2. Lightweight blocks (LWB) production

2.2.1. Mixture composition

The potential incorporation of TW as a raw material to produce lightweight blocks with thermal and non-structural properties for application on partition walls was evaluated. For the mixture's composition, water, Portland limestone cement (CEM II/B-L 32.5N) and TW were used Fig. 3.

For the manufacture of textile-based compositions, a mixture of water and Portland cement was made, at once the TW was introduced until obtaining, as well as possible, a homogeneous mixture. This procedure can be seen in Fig. 4. A release agent was applied to the mold's surface before the mixtures were poured into it.

Different percentages of TW were considered in the mixture composition in order to analyze their influence on the LWB thermal performance. TW percentages were defined focusing on increasing the addition of waste and decreasing the cement content in the mixture, guarantying workability and reducing segregation. Table 1 shows the composition of the mixtures to produce LWB1, LWB2, and LWB3.

Considering the lack of knowledge in this field regarding the mixture performance, particularly in what concerns to workability, water absorption, and its behavior during the curing process, optimization of the mixtures was carried out. The mixture of LWB1 presents the lowest percentage of TW while LWB3 has the highest percentage of TW incorporation. The quantity of cement decreased with the increase of TW but an adjustment in the water percentage was performed. The composition LWB1 was the first mixture to be developed and it was considered as the reference sample. After the curing process, considerable segregation of cement in the specimens with the LWB1 composition was verified. To avoid this phenomenon, this mixture was optimized by reducing the quantity of cement, leading to composition LWB2. Although a reduction in cement segregation was verified after the curing process, it persisted and so, an optimization of the mixture composition

Fig. 3. Materials used in the mixture's composition: TW, water, and Portland cement.

Fig. 4. Preparation of the mixtures: a) Cement and water mixture; b) TW incorporation; c) Final mixture.

Table 1
Composition of the LWB mixtures, in weight percentage (wt%).

Mixture ID	TW (wt%)	Cement (wt%)	Water (wt%)
LWB1	6.25	46.88	46.88
LWB2	8.16	30.61	61.22
LWB3	8.75	32.86	58.40

allowed to obtain LWB3. In this case, the amount of cement was adjusted, and the percentage of water was reduced.

As referred, mixture optimization was performed to avoid segregation and three different compositions were defined. However, the material integrity was verified for the different specimens after the curing process, showing that different degrees of cement segregation could be an advantage for subsequent application in partition walls as coating materials given the regularization of one of the specimen surfaces. Furthermore, the addition of textile wastes with high water absorption to cementitious composites may lead to shrinkage occurrence. However, studies revealed that shrinkage of mortar strongly depends on the type and quantity of wastes incorporated in the mixture, their surface characteristics and moisture absorption behavior [35]. In the particular case of the lightweight blocks, this phenomenon did not occur in a significant way capable of influencing the integrity of the blocks and the analysis of the thermal properties. Thus, despite having proceeded to optimize the mixture's composition avoiding segregation phenomenon, the thermal performance analysis was carried out for the three mixtures, allowing to compare the influence of different percentage of TW on LWB thermal properties.

2.2.2. LWB manufacturing process

Molds with dimensions 60 cm × 25 cm × 10 cm (length × height × width) were made in pinewood, Fig. 5. A specimen was considered for each mixture composition for further thermal behavior analysis. Fig. 6 presents the lightweight blocks LWB1, LWB2, and LWB3 which were demolding after three days.

2.2.3. Density

In Fig. 7, it is represented the mass variation of LWB1, LWB2, and LWB3 during the curing process. It can be observed higher values for the specimen LWB1 when compared to LWB2 and LWB3, which can be justified by the fact that approximately the double amount of cement was used in the first block comparing to the other two. It was verified that after 72 days of curing, LWB1 was 45.3% and 47.8% heavier than LWB2 and LWB3, respectively. The drastic decrement in mass verified for LWB2 and LWB3 results from the TW water absorption capacity during the mixture production, which increases with the increasing of TW content (Table 1). LWB2 and LWB3 present similar proportions for TW, water and cement, leading to similar drying process. LWB1 presented a less accentuated decrement in mass which may result from lower percentage of TW in the mixture, which means that water is essentially used for cement hydration, with a smaller amount being absorbed by the TW when compared to LWB2 and LWB3. It can be also noticed that the mass of all specimens tends to stabilize after 28 days of age.

Most lightweight building blocks are produced with ordinary Portland cement (OPC)-based concrete. Furthermore, a low-density construction material is considered when it has a density between 300 kg/m^3 and 1800 kg/m^3 [36,37]. Table 2 shows the specific mass or density of the studied specimens after 72 days of curing, where it can be observed that LWB3 is the lowest-density unit since the density diminishes as a decreasing cement content and an increasing TW percentage.

2.3. Thermal performance analysis

2.3.1. Experimental setup

Experimental tests were carried out to analyze the lightweight blocks thermal performance. This experimental analysis was performed to estimate the thermal transmission coefficient (*U*) following the procedure according to ISO 9869 (1994) [38], Pereira (2011) [39], and already carried out in similar research works [24,40,41,42,43]. In addition to the calculation of *U* value, data acquired during the measurement period allowed to obtain the oscillation patterns of heat fluxes and surface temperatures for each LWB, leading to their thermal behavior characterization. Experimental work was developed in a test room with 4.00 m × 3.00 m × 2.54 m (length × width × height) size, whose indoor conditions were controlled. A uniform high thermal gradient between indoor and outdoor environments is desirable to guarantee a significant heat flow, always occurring in the same direction across the analyzed samples. In this case, these conditions were achieved heating the test room, guarantying an interior temperature with lower oscillation

Fig. 5. Lightweight blocks mold (60 cm × 25 cm × 10 cm).

Fig. 6. Lightweight blocks: a) LWB1; b) LWB2; c) LWB3.

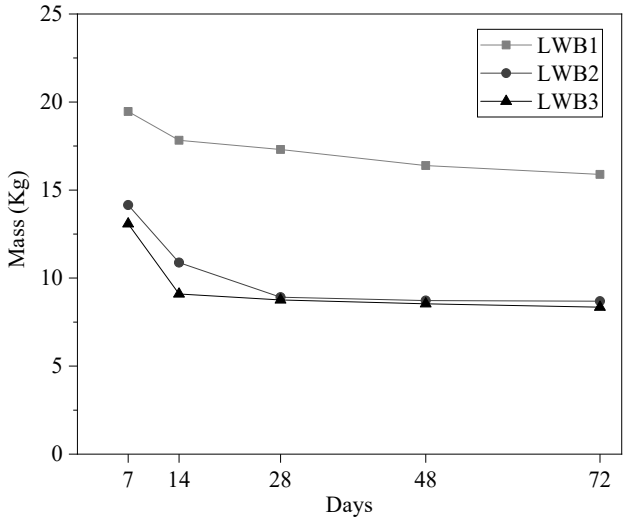

Fig. 7. Drying process of the lightweight blocks.

Table 2
Density of LWB1, LWB2, and LWB3 after 72 days of curing.

Specimen ID	Mass (kg)	Volume (m^3)	Density (kg/m^3)
LWB1	15.89	0.015	1059.07
LWB2	8.69	0.015	579.40
LWB3	8.35	0.015	556.60

patterns and always higher than the outside temperatures. Three panels, each one corresponding to one lightweight block, were analyzed simultaneously, allowing to compare the thermal performance of the different LWB compositions. These panels were placed in the north oriented external wall of the test room, carefully fixed to the external wall, surrounded by extruded polystyrene (XPS) and polyurethane foam (PU) to avoid thermal bridges, non-insulated headers and other faults that could lead to lateral flows occurrence and comprise the experimental test reliability (Fig. 8 and Fig. 9). Fig. 8 shows the different steps for placing the LWB on the XPS panel, properly insulated, for subsequent application on the exterior wall of the test room, as presented in Fig. 9.

The experimental equipment was composed of two heat flux sensors, HF_1 and HF_2, four inner surface temperature sensors, Tsi_{11}, Tsi_{12}, Ts_{21}, and Tsi_{22} fixed in each block (Fig. 10) and two temperature sensors, one inside the test room (*Ti*) and the other outside (*Te*) to measure the exterior environmental conditions. The heat flux and the surface temperature sensors were fixed in the block's inner surface.

The temperatures of the internal and external environments (*Ti(n)* and *Te(n)*), the heat flux (*q1(n)* and *q2(n)*) measured, respectively, by HF_1 and HF_2, and the inner surface temperatures (*Tsi(n)*) were continuously acquired with 10 min' intervals *(n)*.

According to ISO 9869 [38], the measurement period is the time needed to maintain the heat flux signal and it depends on the thermal inertia and the heat storage capacity of the building solution under analysis. In this case, the maintenance of the heat flux signal was guaranteed by heating the test room and achieving an interior temperature always higher than the exterior temperature during the measurement period. ISO 9869 [38] also states that for high inertia elements, a fourteen-day test period is recommended, while for the case of low thermal inertia, measurements can be performed for a minimum period of 72 h. However, a test duration higher than the required has been used in the study of new building components, namely the ones composed of

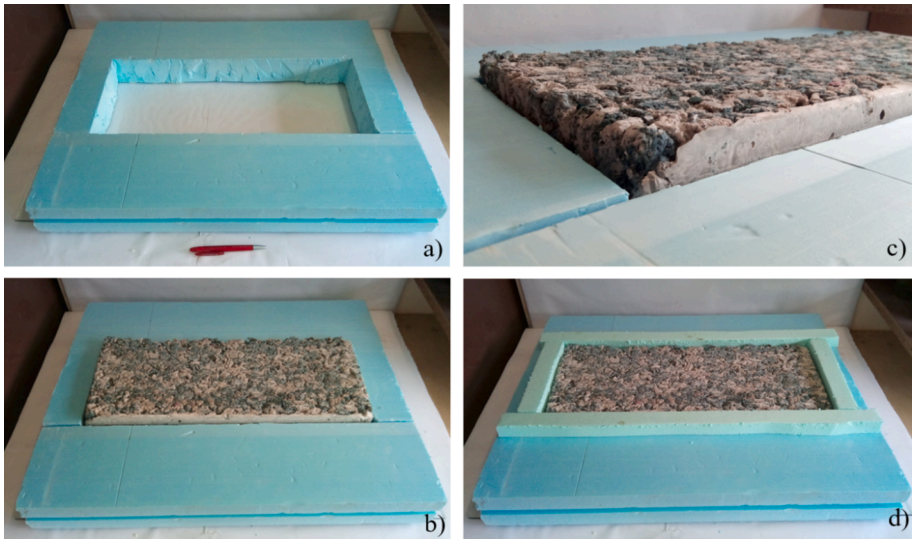

Fig. 8. Sample's preparation: a) XPS panel; b) and c) placement of the LWB; d) placement of insulation boards surrounding the sample.

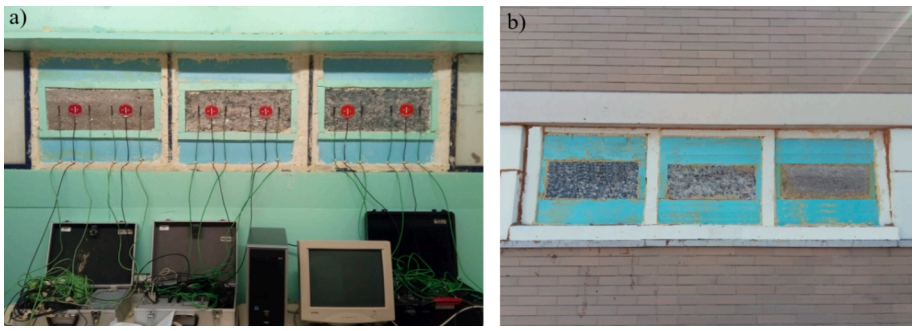

Fig. 9. Experimental setup: a) interior view; b) exterior view.

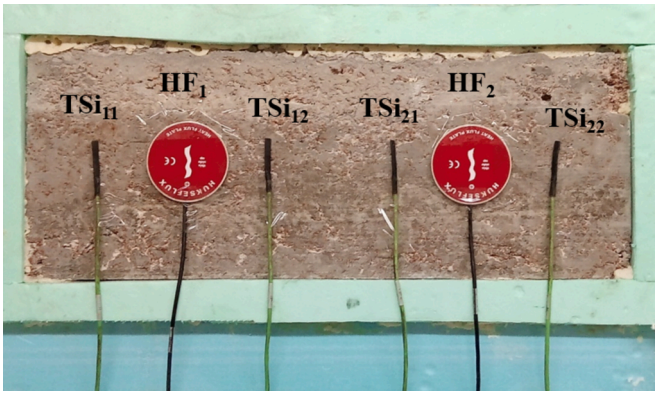

Fig. 10. Sensor's location: Heat flux sensors HF_1 and HF_2; Inner surface temperature sensors Tsi_{11}, Tsi_{12}, $Ts_{21,}$ and Tsi_{22}.

unusual materials or multi-layer systems [40,41]. So, experimental measurements were carried out during 11 days in order to consider the heterogeneity of the textile waste blocks and the test conditions stabilization. The measurement period occurred between the 9th and the 20th of September.

2.3.1.1. Calculation methodology. The ISO 9869 [38] indicates that the measurement of the thermal transmission coefficient (*U*) of a building element using a heat flow meter, assessing temperature in both sides of the building element, can be done assuming that the mean value of the heat flow rate and temperatures over a sufficiently long period of time provides a good estimate of the steady-state conditions. It is also considered that the thermal properties and the heat transfer coefficient of the materials are constant over the range of temperature fluctuation that occurs during the experimental test. It can also be assumed that the change of the amount of heat stored in the building element or material is negligible when compared to the amount of heat going through it. In addition, it is recommended to use interior (*Ti*) and exterior (*Te*) temperatures instead of surface temperatures to determine the thermal transmission coefficient. Taking these conditions into consideration, data acquisition and analysis are based on the average method or dynamic method. Thus, the thermal transmission coefficient (*U*) of the LWB can be quantified given the heat flow that occurs through it when subjected to a temperature differential between indoor and outdoor environments, as presented in Eq. (1):

$$U(ntotal) = \frac{\sum_{n=1}^{ntotal} q(n)}{\sum_{n=1}^{ntotal} (Ti(n) - Te(n))} \quad (1)$$

where *q(n)* is the heat flow across the sample for the instant *n*; *Ti(n)* and *Te(n)* are, respectively, the interior and the exterior temperatures in the instant *n*; *ntotal* refers to the total number of instants in which data was registered during the measurement period.

As referred previously, the heat flux values, *q1(n)* and *q2(n)* are obtained by placing the two heat flux sensors, *HF1* and *HF2*, in each LWB. The use of four temperature sensors in the inner surface of each LWB allows the acquisition of *Tsi11(n)*, *Tsi12(n)*, *Tsi21(n),* and *Tsi21(n)* values. Assessing the temperature differential between the interior, *Ti (n)*, and the exterior, *Te(n)*, environments, it is possible to estimate the thermal transmission coefficients for each LWB panel, *U1(ntotal)* and *U2 (ntotal)*, respectively, by applying Eq. (1). The thermal transmission coefficient of each LWB solution, *U'(ntotal)*, results from the average value of *U1(ntotal)* and *U2(ntotal)*, as defined in Eq. (2):

$$U'(ntotal) \frac{U1(ntotal) + U2(ntotal)}{2} \quad (2)$$

Based on the experimental assessment of *U'(ntotal)* value for each LWB panel, it was possible to estimate the thermal resistance *R'(ntotal)* of the proposed building solution, using Eq. (3).

$$R'(ntotal) = \frac{1}{U'(ntotal)} \quad (3)$$

Considering the external and internal superficial thermal resistances, *Rse* and *Rsi*, respectively, it was possible to obtain the thermal resistance of each LWB, R_{LWB}, by applying Eq. (4). In this case, the values of *Rse* and *Rsi* are 0.04 $m^{2\circ}C/W$ and 0.13 $m^{2\circ}C/W$, respectively [44].

$$R'(ntotal) = R_{LWB} + R_{Si} + R_{Se} \quad (4)$$

Although the LWB homogeneity is conditioned by the percentage and size of the TW pieces incorporated in the mixture's composition, solid blocks with visible integrity were obtained after the curing process, Fig. 11, leading to a theoretical approach on the thermal conductivity value (λ_{LWB}) of the material that makes up each of the LWB, applying Eq. (5).

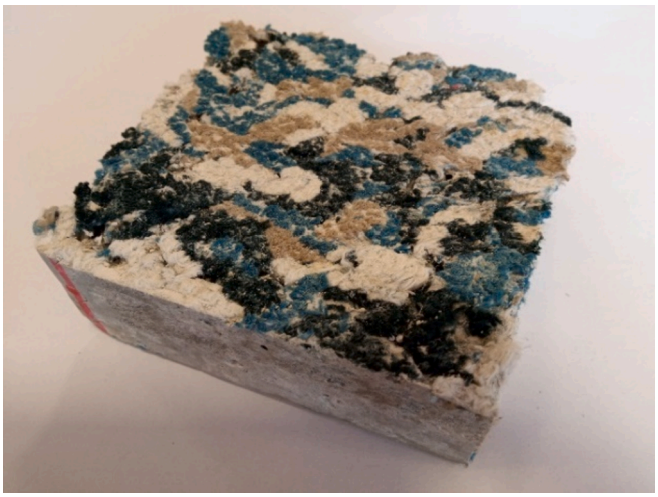

Fig. 11. LWB cutting detail after the curing process.

$$\lambda_{LWB} = \frac{e_{LWB}}{R_{LWB}} \quad (5)$$

where e_{LWB} represents the thickness of lightweight blocks, which in this case is 10 cm and R_{LWB} is the respective thermal resistance, calculated previously according to equation (4).

This calculation methodology was applied for the three analyzed LWB and allowed to estimate the values of the thermal parameters resulting from experimental measurements, which were compared with the values already known for current building solutions with insulation purposes.

A complementary thermographic analysis was also carried out using a thermography camera to identify the surface temperatures fluctuation of the different LWB, both inside and outside, at different periods of the day (10 a.m., 2 p.m., 6 p.m., and 10 p.m.) using infrared technology. The evolution of temperature fluctuations throughout the day in each sample as well as a comparative analysis between the different LWB compositions were performed.

3. Results and discussion

3.1. Heat flux

The experimental measurements allowed to obtain the temperature variation of the indoor and outdoor environments. In Fig. 12, it can be observed that the requirements defined in ISO 9869 [38] were guaranteed in what concerns to the maintenance of the heat flux signal given that heating the room allowed to achieve values of *Ti* always higher than *Te* during the measurement period. A stabilization of *Ti* was obtained with an average value of 35.7 °C. The minimum and the maximum values recorded for *Te* were 7.9 °C and 29.1 °C, respectively. Thus, a positive differential between *Ti* and *Te* was verified during all the test period, where a minimum value of 6.2 °C was obtained during the day and a maximum value of 28.2 °C was achieved during the night. This temperature variation leads to positive curves of *q1(n)* and *q2(n)* during the experimental tests, as shown in Fig. 12.

A comparison between the three LWB panels allowed to conclude that higher values of *q1(n)* and *q2(n)* were verified for the LWB1 solution, with significant variations between the day and the night periods. So, higher oscillation patterns of heat flux curves were identified in the case of LWB1, whose mixture includes lower TW percentage and higher cement content. An average differential around 2.2 W/m^2 was verified between *q1(n)* and *q2(n)* in the case of LWB1, showing that heat flux sensors HF_1 *and* HF_2 were fixed at points of the material with similarities in terms of composition and homogeneity. Values of 0.87 W/m^2 and 4.4 W/m^2 were obtained in the case of LWB2 and LWB3, respectively. It was also found that LWB2 and LWB3 samples presented similar heat flux values since their curves are almost overlaid. However, LWB3 displayed slightly greater oscillations in its curves that may be ascribed to a greater number of empty voids resulting from the decrease of cement quantity and the size of TW pieces, which can also justify a higher average differential between *q1(n)* and *q2(n)* values when compared to the remaining solutions. Comparing the average values of *q1(n)* and *q2(n)* for the three panels, LWB2 and LWB3 presented, respectively, a reduction of 33.8% and 39.5% in the heat flux values when compared to the ones that characterize LWB1. A delay in the peaks of LWB2 and LWB3 curves was also verified in relation to LWB1, showing better resistance to heat transfer in the case of the samples with higher TW content when subjected to the same temperature differential between the indoor and the outdoor environments.

3.2. Inner surface temperatures

The variation of the inner surface temperatures shown in Fig. 13 also corroborates the results presented previously in what concerns to the heat flux variation. Lower values of *Tsi* were obtained for the LWB1 solution and the curves of LWB2 and LWB3 panels are practically overlapped, following similar oscillation patterns to the ones observed in the case of heat flux curves. For each textile waste lightweight block, the values acquired by two inner surface temperature sensors, $Tsi_{11}(n)$ and $Tsi_{21}(n)$, are represented in Fig. 13. The oscillations recorded showed a minimum of 23.8 °C, a maximum of 34.1 °C, and an average value of 32.0 °C in the case of LWB1.

The average temperatures found on the surface of LWB2 and LWB3 are 3.1% higher than the ones verified for the LWB1 solution. In both cases, a minimum and a maximum temperature around 25.0 °C and 33.0 °C, respectively, were registered. However, it is worth noting that their inner surface temperature curves were more regular than the *Tsi* curves of sample LWB1. As stated before, this difference in the thermal behavior of LWB1 comparing with LWB2 and LWB3 can be attributed to the mixture composition, since LWB1 has less than 23.4% of textile waste and more than 34.7% of cement content.

3.3. Thermal transmission coefficient

The acquired values of *Ti(n)*, *Te(n)*, *q1(n),* and *q2(n)* were used to

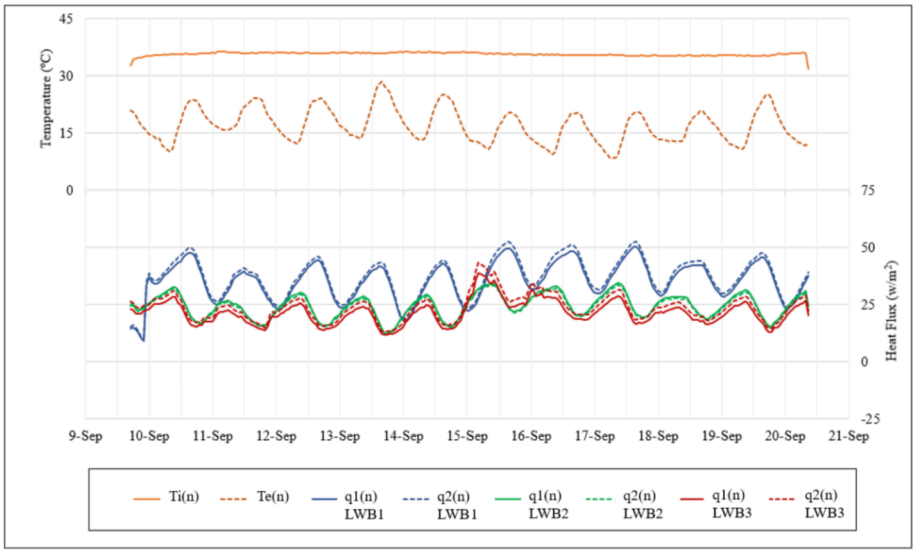

Fig. 12. Variation of interior (*Ti(n)*), exterior (*Te(n)*) temperatures and heat flux (*qi(n)*).

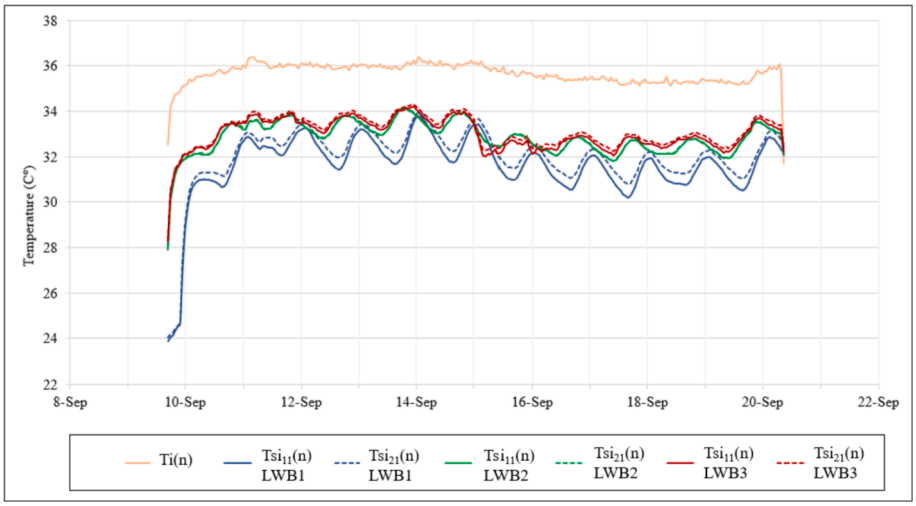

Fig. 13. Variation of interior (*Ti(n)*) and inner surface temperatures (*Tsi(n)*).

estimate the thermal transmission coefficients *U1(ntotal)* and *U2(ntotal)*, Fig. 14, and the average value *U'(ntotal)* for each LWB solution, applying Eq. (1) and Eq. (2). As it can be seen, a stabilization of the thermal transmission coefficient values is verified during the experimental measurement, excluding the beginning and the ending periods of the test period, which are not considered in the calculation of *U'(ntotal)* value. The higher values of *U1(ntotal)* and *U2(ntotal)* correspond to the LWB1 solution, while LWB2 and LWB3 are characterized by the proximity of the thermal transmission coefficient values. According to Eq. (2), *U'(ntotal)* values of 1.98 W/m$^{2\circ}$C, 1.29 W/m$^{2\circ}$C and 1.19 W/m$^{2\circ}$C are estimated for LWB1, LWB2 and LWB3 panels, respectively. It means that the thermal transmission coefficient for LWB2 and LWB3 were 35% and 40%, respectively, lower than LWB1. These results are ascribed to the mixture composition, as was already explained in section 3.2.

The thermal resistance *R'(ntotal)* of each block panel was also calculated using Eq. (3) and the values of 0.51 m$^{2\circ}$C/W, 0.78 m$^{2\circ}$C/W, and 0.84 m$^{2\circ}$C/W were obtained, respectively, for the solutions of LWB1, LWB2, and LWB3. Given the inverse proportionality between the thermal transmission coefficient and the thermal resistance, the LWB1 panel had the lowest thermal resistance in comparison LWB2 and LWB3 solutions, which values are very close. Considering Eq. (4), the thermal resistance of each textile waste lightweight block, R_{LWB}, can be determined. They are characterized by R_{LWB} values of 0.34 m$^{2\circ}$C/W, 0.61 m$^{2\circ}$C/W, and 0.67 m$^{2\circ}$C/W, respectively. Therefore, *R'(ntotal)* for LWB2 and LWB3 registered an increase of 79% and 97%, respectively, in comparison to LWB1, resulting in lower thermal conductivity values, as seen below. This finding is in line with the results found by El Wazna et al., [45] and Patnaik et al., [29] who investigated the thermal properties of nonwoven material based on wool and acrylic, and wool and recycled polyester, respectively.

A theoretical value was also estimated for the thermal conductivity (λ_{LWB}) of each block. Values of 0.294 W/m°C, 0.164 W/m°C and 0.2149 W/m°C were achieved for LWB1, LWB2 and LWB3, respectively. LWB2 and LWB3 results are in accordance with the λ values obtained by Dissanayake [25] in samples with a thickness of 6.0 and 6.6 mm and 20.0 and 22.5 g, of post-industrial textile waste, respectively. This author studied a method to produce heat-insulating materials by compression molding, using postindustrial waste nylon/spandex fabrics and polyurethane offcuts. It is also comparable with Muthuraj's [46] results, who utilized textile waste fiber to develop a lightweight and thermal insulation composite for interior building materials.

The obtained values for the different thermal performance parameters support the reliability of the experimental results since it is in accordance with the percentage of TW used in the composition of the mixtures. In Table 3, the main results of the LWB thermal performance are summarized, presenting the average values for the different variables under analysis.

A comparison of the proposed solutions with currently available

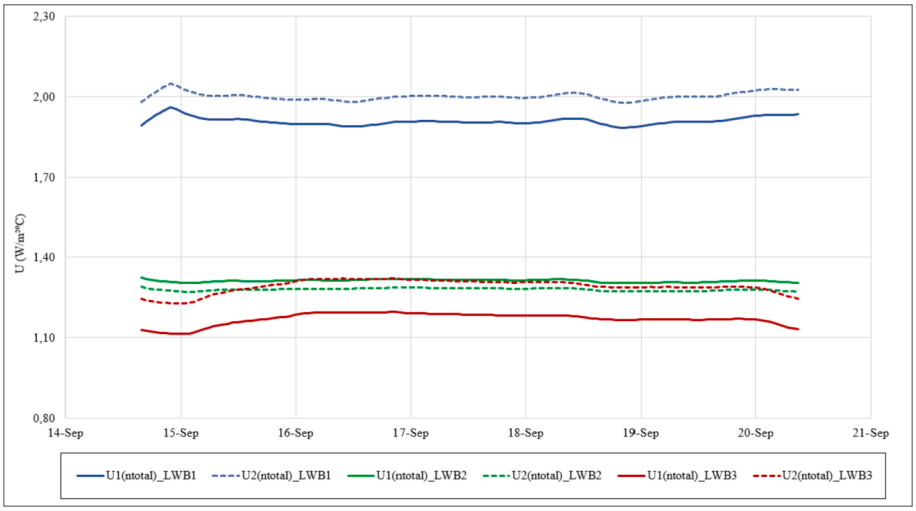

Fig. 14. Variation of the thermal transmission coefficients (U_1*(ntotal)* and U_2*(ntotal)*).

Table 3
Results of the LWB thermal performance assessment.

Panel ID	*Ti* (°C)	*Te* (°C)	*Tsi* (°C)	*qi* (W/m^2)	*U'(ntotal)* (W/m$^{2\circ}$C)	*R'(ntotal)* (m$^{2\circ}$C/W)	R_{LWB} (m$^{2\circ}$C/W)	λ_{LWB} (W/m°C)
LWB1	35.7	16.6	32.0	37.0	1.98	0.51	0.34	0.294
LWB2			32.9	24.5	1.29	0.78	0.61	0.164
LWB3			33.1	22.4	1.19	0.84	0.67	0.149

building materials was also carried out to assess their suitability for thermal insulation purposes. Comparing the thermal resistance values obtained for the three LWB with the values available for simple masonry walls with 10 cm of thickness, it is observed that the proposed blocks present values of the same magnitude, being even higher in the majority of the cases, thus revealing more satisfactory properties in terms of thermal performance, as indicated in Table 4, [44]. For example, considering a common solution of ceramic solid brick, whose thermal resistance value is 0.13 m$^{2\circ}$C/W, higher values can be achieved for all the LWB solutions. This is also verified when a comparison is performed with hollow ceramic bricks or lightweight concrete blocks. In addition, a comparative analysis was done considering the thermal conductivity value. In this case, current insulating concrete forms were compared, showing promising results for the proposed textile waste-based materials.

3.4. Infrared thermal imaging analysis

Thermography is a non-destructive testing technology that can be used to evaluate building performance [47]. It worth to mention that the surface pattern strongly depends on the material properties, i.e. thermal diffusivity, porosity, density [48]. In this study, a thermographic camera was used to analyze the LWB surface temperatures fluctuation at different periods of the day with 4 h' intervals. Different thermograms were collected 2 m away from the samples, considering as input parameters the material emissivity and the reference temperature equal to 0.54 and 20 °C, respectively. In Figs. 15–18, the inner and the outer surface temperatures values, *Tsi* and *Tse*, respectively, are represented for each LWB panel, so a comparison of the temperature profiles can be performed. Table 5 presents the indoor and outdoor environmental conditions regarding the acquired values of air temperature (*Ti* and *Te*) and relative humidity (*HRi* and *HRe*). Infrared thermal imaging can give additional information about the thermal behavior of each sample when submitted to the same temperature gradient and allow to identify possible heterogeneity zones [24] in the LWB composition.

Table 4
Comparison of the thermal performance parameters between LWB and current building solutions [44].

Building solution		*R* (m^2 °C/W)	λ (W/m °C)
Textile waste lightweight blocks (10 cm)	LWB1	0.34	0.294
	LWB2	0.61	0.164
	LWB3	0.67	0.149
Current materials and masonry elements	Hollow ceramic brick (10 cm)	0.27	-
	massive ceramic brick (10 cm)	0.13	-
	concrete blocks	0.16	-
	lightweight concrete blocks	0.27	-
	insulating concrete (ρ= 1000 Kg/m^3)	-	0.36
	cavernous concrete (800 ≤ ρ (Kg/m^3) ≤ 1000)	-	0.33
	cavernous concrete (600 ≤ ρ (Kg/m^3) ≤ 800)	-	0.25
	perlite or expanded vermiculite aggregate concrete (400 ≤ ρ (Kg/m^3) ≤ 600)	-	0.20
	pumice aggregate concrete for masonry blocks (ρ= 500 Kg/m^3)	-	0.16
	expanded polystyrene aggregate concrete (ρ= 600 Kg/m^3)	-	0.22

Fig. 15 shows the thermograms collected during the morning period, at 10 a.m. from the interior and exterior of the test room. Comparing the thermographic images of the three LWB, zones of heterogeneity in LWB3 stand out, represented by darker spots with lower inner surface temperature values, suggesting the existence of a greater number of voids resulting from the increase in the amount of TW and the reduction of cement content in the mixture composition. This heterogeneity is also visible from the thermal images registered outside. In this context, LWB3 is characterized by the highest surface temperatures, in both inner and outer surfaces. The values of *Tsi* are very similar for the LWB1 and LWB2 panels, while for *Tse* values this difference is more pronounced. For all the cases, *Tsi* and *Tse* values are higher than *Ti* and *Te* values, respectively. It is also verified that the temperature differential between *Tsi* and *Tse* for each block is not very significant, which is due to the material thermal properties.

At 2:00 p.m., the second group of thermograms was collected, Fig. 16. During this period of the day, the highest values of *Te* were registered outside, while inside, the temperature value was similar to the ones at the remaining periods of image collection given the temperature stabilization when the room heating was guaranteed. Despite the difficulty in capturing thermograms with proper clarity given the increase in *Te* and *Ti* values, it is possible to verify proximity regarding *Tsi* values, which is more significant in the LWB1 and LWB2 solutions, and slightly higher in the case of LWB3. The surface temperatures outside presented more distant values, where *Tse* value for LWB3 (Fig. 16f) is 9% higher than LWB1 (Fig. 16d) which can be justified by the thermal resistance increase when a higher percentage of textile waste is incorporated in the mixture.

At 6 p.m., the test conditions were practically similar to the previous ones, although a decrease in *Te* value was verified. It was observed that LWB1 presented the highest *Tsi* and *Tse* values, Fig. 17a and d, in contrast to the recorded values at 10 a.m. and 2 p.m. This can be indicative of a higher heat storage capacity of the LWB1 material as it presents a greater cement content in its composition, thus leading to higher thermal inertia and a consequent heat delay. In addition, these results are in accordance with the differences verified in the LWB heat flux curves presented previously in Fig. 12 and with the highest density value of the LWB material. It is also observed a slightly darker color at the bottom of the specimens which can be associated with the materiaĺs segregation at the top. It causes higher surface temperatures due to the lack of cement content, which is replaced by textile waste pieces, and a high number of voids can be created in that zone. This situation is highlighted by a large light spot in the upper right corner of the LWB3 thermal image.

The thermograms taken at 10 p.m. show lower surface temperatures Fig. 18, than the ones registered previously, which is expected given the temperature range between the day and the night periods. All the LWB panels presented lower *Tse* values when compared to *Te* and only LWB1 achieved a slightly higher *Tsi* value comparing with *Ti*. At this time, as was already verified for the registered values at 6 p.m., LWB1 presented the highest *Tsi* and *Tse* values, due to the reasons referred previously. A higher differential between the inner and outer surface temperatures is also verified for all the samples, being more significant in the LWB3 panel, where *Tsi* is 4.3 °C higher than *Tse*.

In Figs. 19 and 20, the values of the LWB inner and outer surface temperatures obtained for all the collecting periods of thermographic imaging are represented. It can be observed that LWB1 is characterized by the greatest surface temperature differential, being the specimen with

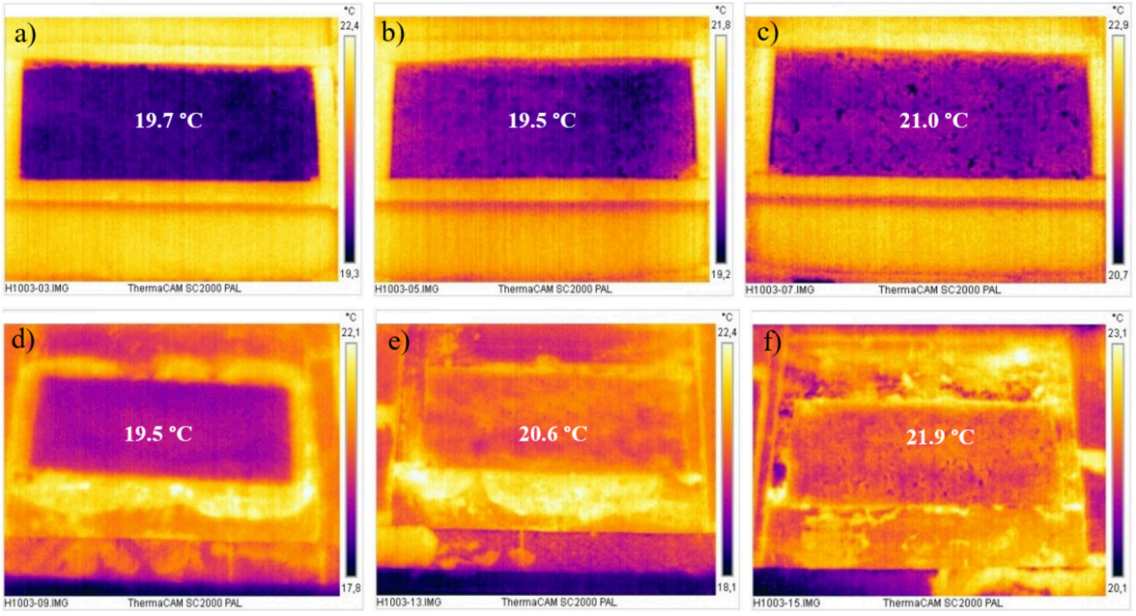

Fig. 15. Thermograms recorded at 10 a.m. inside the test room a) LWB1, b) LWB2, c) LWB3, and outside d) LWB1, e) LWB2, f) LWB3.

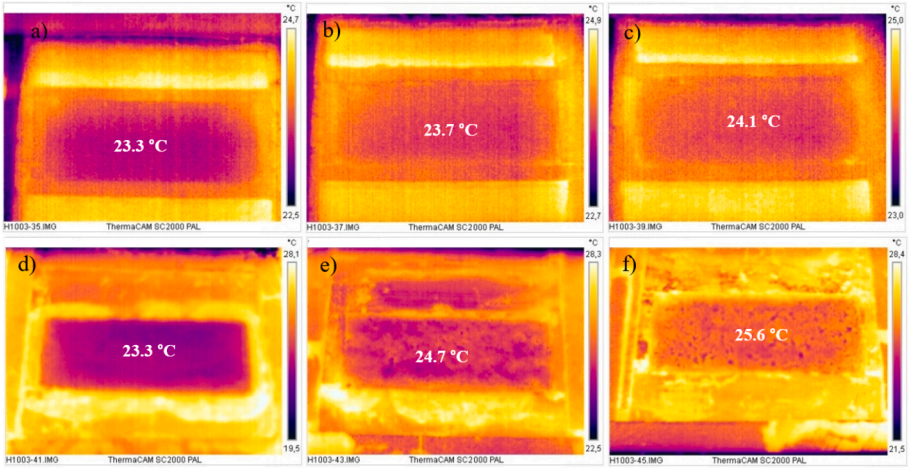

Fig. 16. Thermograms recorded at 2 p.m. inside the test room a) LWB1, b) LWB2, c) LWB3, and outside d) LWB1, e) LWB2, f) LWB3.

less thermal stability, as was already concluded in the thermal behavior experimental tests. The surface temperatures values of LWB2 and LWB3 were also very close, even so, the specimen LWB3 presented surface temperatures consistent with the thermal resistance increasing and the thermal conductivity decreasing.

At 10 a.m., LWB3 showed inner surface temperature values higher than LWB1 and LWB2 in 6.6% and 7.7%, respectively, and a similar trend was registered at 2 p.m. However, at 6 p.m., an increase of 2.6% and 3.8% was recorded for LWB1compared to LWB2 and LWB3, while at 10 p.m. values of 2.2% and 2.6% were, respectively, achieved. Similar behavior was observed for outer surface temperatures registered during the day. So, greater TW content leads to a better space heating in the early hours of the day, which indicates that LWB3 sample was the slowest to cool down overnight. This suggests that with a higher TW percentage in the lightweight block composition, a better thermal stability can be achieved, as it can be observed in the case of LWB3. The obtained results are in accordance with the findings of Nermin [49] who studied the acoustic and thermal performance of sustainable fiber reinforced thermoplastic composite panels for buildings insulation using three types of recycled nonwoven fabrics (jute 100%, polyester (PET) 100%, and hybrid jute-polyester (80:20%)).

4. Conclusions

The thermal performance characterization of cement-based lightweight blocks incorporating different percentages of textile waste (TW) was performed in order to evaluate their suitability as insulation materials purposes. TW percentages of 6.25%, 8.16%, and 8.75% were considered in the cement mixture composition of LWB1, LWB2 and LWB3, respectively so their influence on the LWB thermal performance could be discussed. The TW under study was fabric leftovers from the textile industry, composed by 70% wool, 25% viscose, and 5% elastane, which was cut into smaller pieces before the LWB manufacturing to ensure the mixture workability and homogeneity as much as possible. The LWB thermal performance characterization was carried out by analyzing heat fluxes, inner surface temperatures, thermal transmission coefficients, and infrared thermal imaging. Experimental measurements showed that higher oscillation patterns of heat flux and inner surface temperature curves were verified for LWB1, whose mixture includes a lower weight percentage of TW and higher cement content. Values of

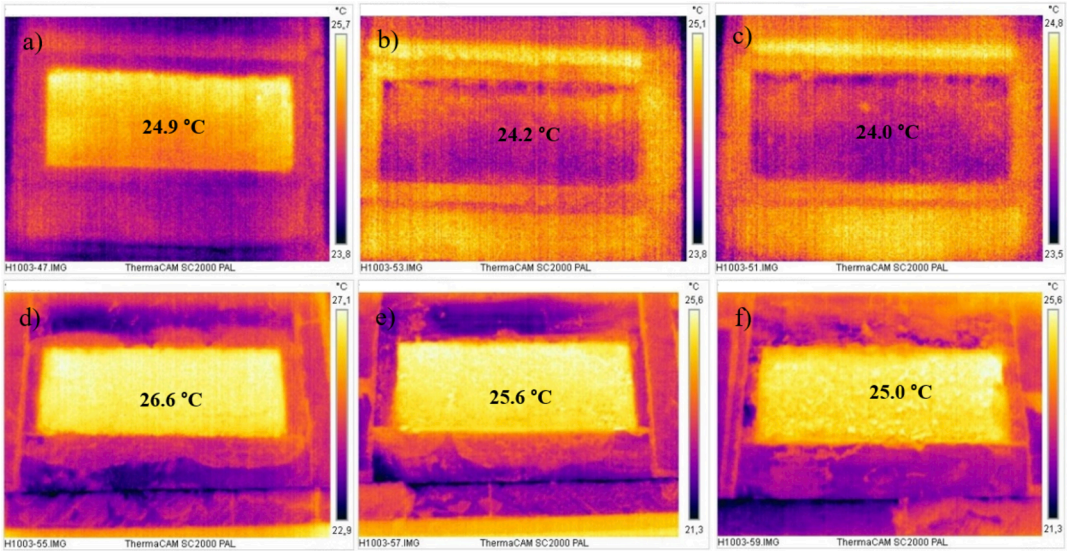

Fig. 17. Thermograms recorded at 6 p.m. inside the test room a) LWB1, b) LWB2, c) LWB3, and outside d) LWB1, e) LWB2, f) LWB3.

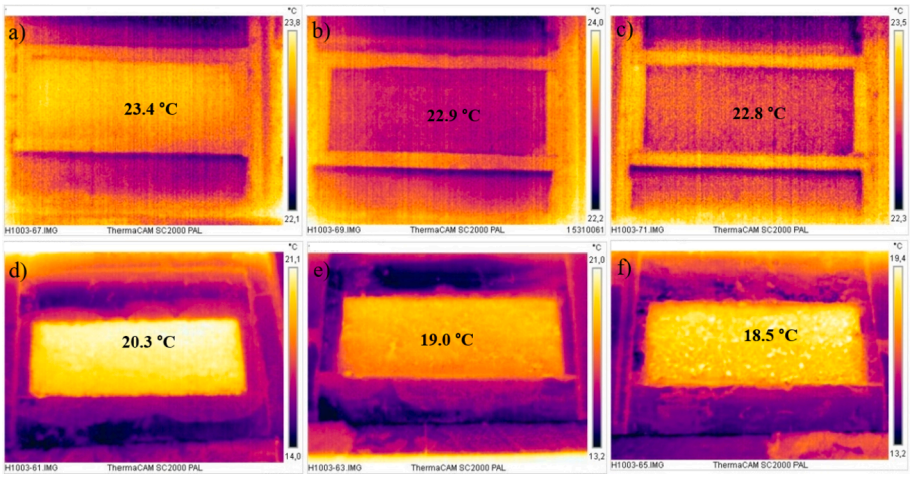

Fig. 18. Thermograms recorded at 10 p.m. inside the test room a) LWB1, b) LWB2, c) LWB3, and outside d) LWB1, e) LWB2, f) LWB3.

Table 5
Environmental conditions during the thermography test.

	10 a.m.	2 p.m.	6 p.m.	10 p.m.
Ti (°C)	22.6	23.1	23.3	23.3
HRi (%)	59.0	54.0	43,9	48.1
Te (°C)	23.2	31.0	25.2	22.6
HRe (%)	60.0	24.0	35.4	43.0

0.34 m^2°C/W, 0.61 m^2°C/W, and 0.67 m^2°C/W were estimated for the thermal resistance of LWB1, LWB2 and LWB3, respectively. So, a thermal resistance increase is achieved when a higher percentage of TW is incorporated in the mixture composition. Furthermore, a water decrease contributed to overcome the segregation problems at an early curing stage.

Based on the experimental results, a theoretical value was also estimated for the thermal conductivity of each LWB. Values of 0.294 W/m°C, 0.164 W/m°C and 0.2149 W/m°C were achieved for LWB1, LWB2 and LWB3, respectively.

A thermal imaging analysis allowed to identify the LWB thermal behavior during different periods of the day, showing with more detail heterogeneity zones and the inner and outer surface temperatures variation. The infrared thermal images confirmed that LWB1 showed a significant thermal instability, while LWB2 and LWB3 presented rather close surface temperatures and a lower temperature differential when compared to LWB1, which is due to the thermal resistance increase when a higher percentage of TW is included in the cementitious mixture composition.

A comparison of the lightweight blocks with commonly used building solutions, such as simple masonry walls and insulating concrete forms, was also performed showing promising results of the proposed textile waste-based materials when applied with insulation purposes.

As this is a preliminary study regarding the possibility of adding textile wastes in the composition of cement-based lightweight blocks, further research work should be developed to evaluate with more detail other physical and mechanical properties of the proposed products, such as mechanical strength, fire behavior and acoustic insulation.

However, the obtained results show the potential use of textile waste as building insulation materials components, contributing to the reduction of energy consumption employed in the exploitation of natural resources, performing a significant role in sustainability, including the environmental, economic, and social perspectives, and fitting the circular economy principles.

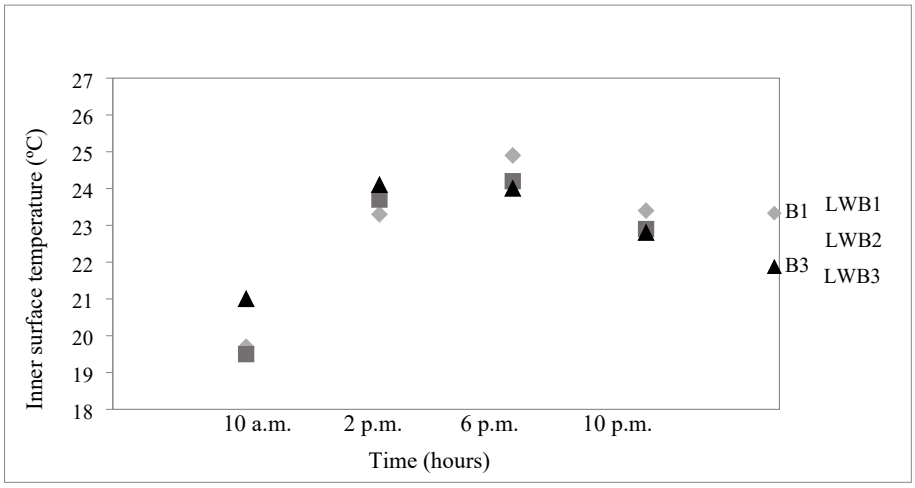

Fig. 19. Inner surface temperatures (*Tsi*) obtained by infrared thermal imaging.

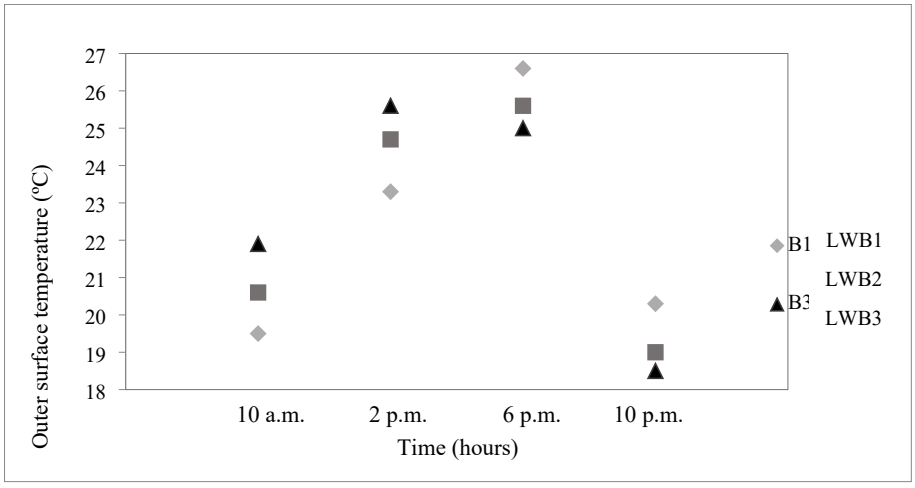

Fig. 20. Outer surface temperatures (*Tse*) obtained by infrared thermal imaging.

CRediT authorship contribution statement

Ana Briga-Sá: Conceptualization, Methodology, Validation, Formal analysis, Investigation, Resources, Data curation, Writing – original draft, Writing – review & editing, Visualization, Supervision. **Norma Gaibor:** Formal analysis, Writing – original draft. **Leandro Magalhães:** Conceptualization, Methodology, Validation, Formal analysis, Investigation, Resources, Data curation. **Tiago Pinto:** Conceptualization, Methodology, Validation, Formal analysis, Investigation, Resources, Data curation, Supervision. **Dinis Leitão:** Methodology, Validation, Formal analysis.

Declaration of Competing Interest

The authors declare that they have no known competing financial interests or personal relationships that could have appeared to influence the work reported in this paper.

References

[1] L.J.R. Nunes, J.C.O. Matias, J.P.S. Catalão, Analysis of the use of biomass as an energy alternative forthePortuguese textile dyeing industry, Energy 84 (2015) 503–508, https://doi.org/10.1016/j.energy.2015.03.052.
[2] L.J.R. Nunes, R. Godina, J.C.O. Matias, J.P.S. Catalão, Economic and environmental benefits of using textile waste for the production of thermal energy, J. Clean. Prod. 171 (2018) 1353–1360, https://doi.org/10.1016/j.jclepro.2017.10.154.
[3] J. Anglade, E. Benavente, J. Rodríguez, A. Hinostroza, Use of textile waste as an addition in the elaboration of an ecological concrete block, IOP Conf. Ser.: Mater. Sci. Eng. 1054 (1) (2021) 012005, https://doi.org/10.1088/1757-899X/1054/1/012005.
[4] S. Yousef, M. Tatariants, M. Tichonovas, L. Kliucininkas, S.-I. Lukošiūtė, L. Yan, Sustainable green technology for recovery of cotton fibers and polyester from textile waste, J. Clean. Prod. 254 (2020) 120078, https://doi.org/10.1016/j.jclepro.2020.120078.
[5] C. Rubino, M. B. Aracil, S. Liuzzi, F. Martellotta, "Preliminary investigation on the acoustic properties of absorbers made of recycled textile fibers," 2019.
[6] E. Tomovska, S. Jordeva, D. Trajković, K. Zafirova, Attitudes towards managing post-industrial apparel cuttings waste, J. Text. Inst. 108 (2) (2017) 172–177, https://doi.org/10.1080/00405000.2016.1160764.
[7] P. Sadrolodabaee, J. Claramunt, M. Ardanuy, A.d.l. Fuente, Characterization of a textile waste nonwoven fabric reinforced cement composite for non-structural building components, Constr. Build. Mater. 276 (2021) 122179.
[8] S. Tedesco, E. Montacchini, From Textile Waste to Resource: A Methodological Approach of Research and Experimentation, *Sustain. 2020, Vol. 12, Page 10667*, vol. 12, no. 24, p. 10667, Dec. 2020, doi: 10.3390/SU122410667.
[9] S. Yousef, M. Tatariants, M. Tichonovas, Z. Sarwar, I. Jonuškienė, L. Kliucininkas, A new strategy for using textile waste as a sustainable source of recovered cotton, Resour. Conserv. Recycl. 145 (2019) 359–369, https://doi.org/10.1016/j.resconrec.2019.02.031.
[10] G. Hole, A.S. Hole, Improving recycling of textiles based on lessons from policies for other recyclable materials: a minireview, Sustainable Prod. Consumption 23 (2020) 42–51.
[11] N.P. Tran, C. Gunasekara, D.W. Law, S. Houshyar, S. Setunge, A. Cwirzen, Comprehensive review on sustainable fiber reinforced concrete incorporating recycled textile waste, J. Sustain. Cem. Mater. (2021), https://doi.org/10.1080/21650373.2021.1875273.

[12] M.P. Todor, I. Kiss, V.G. Cioata, Development of fabric-reinforced polymer matrix composites using bio-based components from post-consumer textile waste, Mater. Today Proc. 45 (2021) 4150–4156, https://doi.org/10.1016/J.MATPR.2020.11.927.
[13] G. Sandin, G.M. Peters, Environmental impact of textile reuse and recycling – a review, J. Cleaner Prod. 184 (2018) 353–365.
[14] I. S. T. (IST) and A. P. do A. (APA), "Guia Sectorial - Textil by Net Resíduos." https://issuu.com/netresiduos/docs/guia_sectorial_textil (accessed May 30, 2020).
[15] H. Cruz, A.C. Broega, M. Amorim, Sustainability in Fashion: A Study of Clean Waste Management within a Clothing Company, Univ. Minho, 2018.
[16] EU, "Directive 2008/98/EC of the European Parliament and of the Council of 19 November 2008 on Waste and Repealing Certain Directives (Waste Framework Directive)." https://ec.europa.eu/environment/waste/framework/ (accessed May 30, 2020).
[17] EU, "Council Decision 2003/33/EC of 19 December 2002 establishing criteria and procedures for the acceptance of waste at landfills persuant to Article 16 of and Annex II to Directive 1999/31/EC Offic. J. Eur. Commun., 16 (2003), p. L11." https://eur-lex.europa.eu/legal-content/EN/TXT/?uri=uriserv:OJ.L_.2003.011.01.0027.01.ENG (accessed May 30, 2020).
[18] EU, "Directive 1999/31/EC on the landfill of waste Off. J. Eur. Communities - Legislation, 182 (1999), pp. 1-19." https://eur-lex.europa.eu/legal-content/EN/TXT/?uri=CELEX%3A31999L0031 (accessed May 30, 2020).
[19] EU, "Directive 2000/76/EC of the european parliament and of the council of 4 december 2000 on the incineration of waste Off. J. Eur. Communities - Legislation, 332 (2000), pp. 91-111." https://ec.europa.eu/environment/waste/legislation/a.htm (accessed May 30, 2020).
[20] S.T. Wagland, F. Veltre, P.J. Longhurst, Development of an image-based analysis method to determine the physical composition of a mixed waste material, Waste Manag. 32 (2) (2012) 245–248, https://doi.org/10.1016/j.wasman.2011.09.019.
[21] G.C. de Oliveira Neto, J.M. Ferreira Correia, P.C. Silva, A.G. de Oliveira Sanches, W.C. Lucato, Cleaner Production in the textile industry and its relationship to sustainable development goals, J. Clean. Prod. 228 (2019) 1514–1525.
[22] P. Sadrolodabaee, J. Claramunt, M. Ardanuy, A. de la Fuente, Mechanical and durability characterization of a new textile waste micro-fiber reinforced cement composite for building applications, Case Stud. Constr. Mater. 14 (2021) e00492.
[23] Y. Ming, P. Chen, L. Li, G. Gan, G. Pan, "A comprehensive review on the utilization of recycled waste fibers in cement-based composites," *Mater. 2021, Vol. 14, Page 3643*, vol. 14, no. 13, p. 3643, Jun. 2021, doi: 10.3390/MA14133643.
[24] A. Briga-Sá, D. Nascimento, N. Teixeira, J. Pinto, F. Caldeira, H. Varum, A. Paiva, Textile waste as an alternative thermal insulation building material solution, Constr. Build. Mater. 38 (2013) 155–160, https://doi.org/10.1016/j.conbuildmat.2012.08.037.
[25] D.G.K. Dissanayake, D.U. Weerasinghe, K.A.P. Wijesinghe, K.M.D.M.P. Kalpage, Developing a compression moulded thermal insulation panel using postindustrial textile waste, Waste Manag. 79 (2018) 356–361, https://doi.org/10.1016/j.wasman.2018.08.001.
[26] A. Gounni, M.T. Mabrouk, M. El Wazna, A. Kheiri, M. El Alami, A. El Bouari, O. Cherkaoui, Thermal and economic evaluation of new insulation materials for building envelope based on textile waste, Appl. Therm. Eng. 149 (2019) 475–483, https://doi.org/10.1016/j.applthermaleng.2018.12.057.
[27] S. Islam, G. Bhat, Environmentally-friendly thermal and acoustic insulation materials from recycled textiles, J. Environ. Manage. 251 (2019) 109536, https://doi.org/10.1016/j.jenvman.2019.109536.
[28] U.H. Erdogan, Y. Seki, F. Selli, "Wool fibres", in: Handbook of Natural Fibres, Elsevier, 2020, pp. 257–278.
[29] A. Patnaik, M. Mvubu, S. Muniyasamy, A. Botha, R.D. Anandjiwala, Thermal and sound insulation materials from waste wool and recycled polyester fibers and their biodegradation studies, Energy Build. 92 (2015) 161–169, https://doi.org/10.1016/j.enbuild.2015.01.056.
[30] A. Abdou, I. Budaiwi, The variation of thermal conductivity of fibrous insulation materials under different levels of moisture content, Constr. Build. Mater. 43 (2013) 533–544, https://doi.org/10.1016/j.conbuildmat.2013.02.058.
[31] L.i. Shen, M.K. Patel, Life Cycle Assessment Of Polysaccharide Materials: A Review, J Polym Environ 16 (2) (2008) 154–167.
[32] X.S. Zhang, Y.Z. Xia, M.W. Shi, X. Yan, The flame retardancy of alginate/flame retardant viscose fibers investigated by vertical burning test and cone calorimeter, Chinese Chem. Lett. 29 (3) (2018) 489–492, https://doi.org/10.1016/j.cclet.2017.07.023.
[33] T. Paunikallio, M. Suvanto, T.T. Pakkanen, Composition, tensile properties, and dispersion of polypropylene composites reinforced with viscose fibers, J. Appl. Polym. Sci. 91 (4) (2004) 2676–2684, https://doi.org/10.1002/app.13450.
[34] S. Korte, C. Siiling, "United States Patent (19) Frauendorf et al. (54) PROCESS FOR PRODUCING ELASTANE FIBERS OF HIGH ELASTICITY AND STRENGTH 75) Inventors: Beatrix Frauendorf, Leverkusen," 1991.
[35] S. Parveen, S. Rana, R. Fangueiro "Macro- and nanodimensional plant fiber reinforcements for cementitious composites", Sustainable and Nonconventional Construction Materials using Inorganic Bonded Fiber Composites, Editor(s): Holmer Savastano Junior, Juliano Fiorelli, Sergio Francisco dos Santos, Woodhead Publishing, 2017, pp. 343-382, ISBN 9780081020012, doi: 10.1016/B978-0-08-102001-2.00020-6.
[36] P. Posi, C. Teerachanwit, C. Tanutong, S. Limkamoltip, S. Lertnimoolchai, V. Sata, P. Chindaprasirt, Lightweight geopolymer concrete containing aggregate from recycle lightweight block, Mater. Des. 52 (2013) 580–586, https://doi.org/10.1016/j.matdes.2013.06.001.
[37] D. Castañeda, G. Silva, J. Salirrosas, S. Kim, B. Bertolotti, J. Nakamatsu, R. Aguilar, Production of a lightweight masonry block using alkaline activated natural pozzolana and natural fibers, Constr. Build. Mater. 253 (2020) 119143, https://doi.org/10.1016/j.conbuildmat.2020.119143.
[38] ISO 9869, ISO 9869. Thermal insulation – building elements – in-situ measurement of thermal resistance and thermal transmittance. International Organization for Standardization (ISO). 1994.
[39] S. Cunha, "In situ evaluation and certification of the thermal quality of residential buildings" (in Portuguese), 2011, PhD Thesis, UTAD, Vila Real, Portugal.
[40] A.B. Sá, S. Pereira, N. Soares, J. Pinto, J.C. Lanzinha, A. Paiva, An approach on the thermal behaviour assessment of tabique walls coated with schist tiles: Experimental analysis, Energy Build. 117 (2016) 11–19, https://doi.org/10.1016/J.ENBUILD.2016.02.016.
[41] A. Paiva, S. Pereira, A. Sá, D. Cruz, H. Varum, J. Pinto, A contribution to the thermal insulation performance characterization of corn cob particleboards, Energy Build. 45 (2012) 274–279, https://doi.org/10.1016/J.ENBUILD.2011.11.019.
[42] D. Leitão, J. Barbosa, E. Soares, T. Miranda, N. Cristelo, A. Briga-Sá, Thermal performance assessment of masonry made of ICEB's stabilised with alkali-activated fly ash, Energy Build. 139 (2017) 44–52, https://doi.org/10.1016/j.enbuild.2016.12.068.
[43] T. Miranda, R.A. Silva, D.V. Oliveira, D. Leitão, N. Cristelo, J. Oliveira, E. Soares, ICEBs stabilised with alkali-activated fly ash as a renewed approach for green building: exploitation of the masonry mechanical performance, Constr. Build. Mater. 155 (2017) 65–78, https://doi.org/10.1016/j.conbuildmat.2017.08.045.
[44] C. Santos, L. Matias, "Coeficientes de Transmissão Térmica de Elementos da Envolvente dos Edifícios Coleção Edifícios – ITE 50," Lisbon, ISBN: 978-972-49-2065-8, 2006. Accessed: Sep. 20, 2021. [Online]. Available: http://home.fa.utl.pt/~lcaldas/LNEC_ITE_50.pdf.
[45] M. El Wazna, M. El Fatihi, A. El Bouari, O. Cherkaoui, Thermo physical characterization of sustainable insulation materials made from textile waste, J. Build. Eng. 12 (2017) 196–201.
[46] R. Muthuraj, C. Lacoste, P. Lacroix, A. Bergeret, Sustainable thermal insulation biocomposites from rice husk, wheat husk, wood fibers and textile waste fibers: Elaboration and performances evaluation, Ind. Crops Prod. 135 (2019) 238–245, https://doi.org/10.1016/j.indcrop.2019.04.053.
[47] E. Barreira, V.P. de Freitas, Evaluation of building materials using infrared thermography, Constr. Build. Mater. 21 (1) (2007) 218–224, https://doi.org/10.1016/J.CONBUILDMAT.2005.06.049.
[48] C. Meola, G.M. Carlomagno, L. Giorleo, The use of infrared thermography for materials characterization, J. Mater. Process. Technol. 155–156 (1–3) (2004) 1132–1137, https://doi.org/10.1016/J.JMATPROTEC.2004.04.268.
[49] N.M. Aly, H.S. Seddeq, K.h. Elnagar, T. Hamouda, Acoustic and thermal performance of sustainable fiber reinforced thermoplastic composite panels for insulation in buildings, J. Build. Eng. 40 (2021) 102747.